

# Continuous weak measurement of the macroscopic quantum coherent oscillations

D.V. Averin

*Department of Physics and Astronomy, SUNY at Stony Brook, Stony Brook, NY 11794-3800*

(October 28, 2018)

The problem of continuous quantum measurement of coherent oscillations in an individual quantum two-state system is studied for a generic model of the measuring device. It is shown that for a symmetric detector, the signal-to-noise ratio of the measurement, defined as the ratio of the amplitude of the oscillation line in the output spectrum to background noise, is independent of the coupling strength between oscillations and the detector, and is equal to  $(\hbar/\epsilon)^2$ , where  $\epsilon$  is the detector energy sensitivity. The fundamental quantum limit of 4 imposed by this result on the signal-to-noise ratio of the measurement with an “ideal” quantum-limited detector reflects the general tendency of a quantum measurement to localize the system in one of the eigenstates of the measured observable. These results are applied to specific measurements of the quantum oscillations of magnetic flux with a dc SQUID, and oscillations of charge measured with a Cooper-pair electrometer. They are also used to calculate the energy sensitivity of a quantum point contact as detector.

## I. INTRODUCTION

Quantum superposition of macroscopically distinct states is one of the most characteristic features of quantum behavior at the macroscopic level. In the “mesoscopic” regime, when the states involved in the superposition correspond to a collective motion of a number of particles that is larger than one but not quite macroscopic, the superposition of states has been demonstrated for photons in a high-quality microwave cavity<sup>1</sup>, and for the center-of-mass motion of large molecules<sup>2</sup>. Among the most basic dynamic manifestations of quantum superposition of states are quantum coherent oscillations between the two basis states of a two-state system. However, while the macroscopic quantum phenomena brought about by the incoherent quantum tunneling are by now commonly found in a variety of systems ranging from mesoscopic tunnel junctions in the regimes of flux<sup>3,4</sup> and charge<sup>5,6</sup> dynamics, to molecular<sup>7,8</sup> and nano-magnets<sup>9</sup>, the situation with experimental observation of macroscopic quantum coherent (MQC) oscillations remains much more uncertain. Claim of the observation of the MQC oscillations in molecular magnets<sup>12</sup> remain highly controversial<sup>13,14</sup>. Remarkable experimental demonstration<sup>10</sup> of the MQC oscillations in the charge-dynamics regime of a small Josephson junction is open to criticism that the two charge states of the observed quantum superposition differ in charge only by the charge of one Cooper pair, and the oscillations between these two states can not be interpreted as macroscopic. Although this criticism is not fully justified, since the charge dynamics of a small Josephson junction is just another representation of its flux dynamics, which is the paradigm of the “macroscopic” quantum dynamics<sup>11</sup>, it does not allow to consider the question of MQC oscillations to be completely settled.

Recently, macroscopic quantum dynamics has attracted renewed attention as the possible basis for de-

velopment of scalable quantum logic circuits for quantum computation. In this context, macroscopic quantum two-state system plays the role of a qubit, an elementary building block of a quantum computer. Several variants of qubits and quantum logic gates have been proposed<sup>15–18</sup> that are based on the macroscopic quantum dynamics of Josephson junctions. Many characteristics of the macroscopic qubits compare favorably with those of the microscopic qubits: they are insensitive to disorder at the microscopic level and offer much larger freedom in design and fabrication of complex systems of qubits. The price of these advantages is the problem of the environment-induced decoherence, which is typically much more serious for the macroscopic than microscopic quantum systems. Suppression of decoherence to the acceptable level requires thorough isolation of the qubit from its environment, the condition that typically limits the ability to control the qubit dynamics.

This trade-off between the external control and decoherence in a qubit has a fundamental aspect related to measurement. Even in the case of a perfect set-up, the measurement necessary to observe the MQC oscillations perturbs the system by projecting its state on the eigenstates of the measured observable, and therefore presents an unavoidable source of decoherence. The intensity of this measurement-induced decoherence increases with increasing coupling strength between the detector and the oscillations, and more efficient measurement leads to stronger decoherence. First approaches to the problem of measurement of the MQC oscillations in an individual two-states system<sup>11,19–21</sup> suggested for oscillations of magnetic flux in SQUIDs, considered only the conventional limit of strong or “projective” quantum measurements, in which the detector-oscillation coupling is strong. In this case, the measurement leads to rapid localization of the measured observable (flux) in one of its eigenstates, and suppresses the oscillation. This means that the time evolution of oscillations can be studied with strong measurements only if the detector can be switched

on and off on the time scale shorter than the oscillations period, and only in the “ensemble” of measurements, i.e. when the experiment is repeated many times with the same initial conditions. The measurement cycle consists then of preparation of the initial state of the system followed by its free evolution and the subsequent measurement. The information about dynamics of the oscillation is contained in the probability distribution of the measurement outcomes. Since the oscillation frequency is limited from below by several factors including the decoherence rate and temperature, the need to switch the detector on and off rapidly in this approach presents at the very least a serious technical challenge.

The goal of this work is to study quantitatively a new approach to measurement of the MQC oscillations that is based on weak quantum measurements<sup>22–24</sup>, in which the dynamic interaction between the detector and the measured system is weak and does not establish perfect correlation between their states. Such a weak measurement provides only limited information about the system but, in contrast to strong measurements, perturbs the system only slightly and can be performed continuously. In this work, the process of continuous weak measurement of the MQC oscillations in an individual two-state system is considered quantitatively. Recent results<sup>25</sup> for continuous measurements of electron oscillations in coupled quantum dots by a quantum point-contact are reformulated within a generic detector model and applied explicitly to the MQC oscillations of flux measured by a dc SQUID and oscillations of charge measured with a Cooper-pair electrometer. It is shown that the signal-to-noise ratio of the measurement, defined as the ratio of the amplitude of the oscillation line in the output spectrum of the detector to the background noise, is fundamentally limited by the trade-off between the acquisition of information and dephasing due to detector backaction on the oscillations. This limitation is the least restrictive for a symmetric detector, for which the signal-to-noise ratio can be expressed as  $(\hbar/\epsilon)^2$ , where  $\epsilon$  is the detector energy sensitivity. Since the energy sensitivity  $\epsilon$  is limited for regular (non-QND) quantum measurements by  $\hbar/2$ , the signal-to-noise ratio of the continuous weak measurement of the quantum coherent oscillations is limited by 4. This limit reflects the fundamental tendency of quantum measurement to localize the system in one of the eigenstates of the measured observable. As a spin-off, the established relation between the signal-to-noise ratio and energy sensitivity is used to demonstrate that the quantum point contact is the quantum-limited detector with energy sensitivity  $\epsilon = \hbar/2$ .

## II. CONTINUOUS MEASUREMENT OF THE MQC OSCILLATIONS WITH A LINEAR DETECTOR

We consider the MQC oscillations in an individual two-states system, with the two basis states separated in en-

ergy by  $\epsilon$  and coupled by the tunneling amplitude  $-\Delta/2$ . The basis states are chosen to coincide with the eigenstates of an oscillating variable  $x$ , for instance, magnetic flux in a SQUID loop. In this basis,  $x = x_0\sigma_z/2$ , where  $x_0$  is the difference between the values of  $x$  in the two states of the system, and  $\sigma_z$  is the Pauli matrix. In the simplest measurement scheme considered in this work, the detector measures directly the oscillating variable  $x$ , and therefore is coupled to  $x$ . This means that the Hamiltonian describing the measurement set-up (Fig. 1) is:

$$H = -\frac{1}{2}(\epsilon\sigma_z + \Delta\sigma_x + \sigma_z f) + H_0, \quad (1)$$

where  $H_0$  is the Hamiltonian of the detector, and  $f$  is the detector operator that couples it to the oscillations. For convenience, the amplitude  $x_0$  of the oscillations and the coupling strength are included in  $f$ .

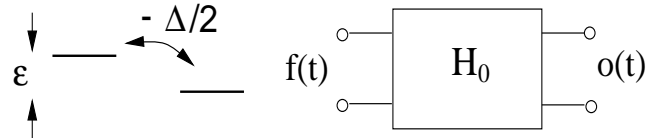


FIG. 1. The diagram of the MQC oscillations in an individual two-state system measured by a linear detector. Detector with the Hamiltonian  $H_0$  is weakly coupled through the operator  $f$  to the oscillating coordinate of the system. The detector output  $o(t)$  consists of noise and linear response to the input oscillations.

We assume that the characteristic response time of the detector is short, e.g., much shorter than the period of measured oscillations, and that the detector operates in the linear regime. These two assumptions mean that the detector output  $o(t)$  can be written as

$$o(t) = q(t) + \frac{\lambda}{2}\sigma_z(t), \quad (2)$$

where  $q(t)$  is the noise part of the output, and  $\lambda$  is a response coefficient. The linearity assumption implies that the coupling  $-\sigma_z f/2$  of the detector to the oscillations is sufficiently weak so that the detector response can be described in the linear-response approximation:

$$\lambda = i \int_0^\infty d\tau e^{i\omega\tau} \langle [q(\tau), f] \rangle_0. \quad (3)$$

The average  $\langle \dots \rangle_0$  in eq. (3) is taken over the stationary density matrix of the detector. Since the response coefficient  $\lambda$  is independent of frequency  $\omega$ , eq. (3) can be written in terms of the  $q$ - $f$  correlator as

$$\langle q(t + \tau) f(t) \rangle_0 = 2\pi S_{qf} \delta(\tau - 0), \quad S_{qf} \equiv \frac{a - i\lambda}{4\pi}, \quad (4)$$

where the infinitesimal shift in the argument of the  $\delta$ -function represents small but finite response time of the

detector, and is needed to resolve the ambiguity in eq. (3). Parameter  $a$  in eq. (4) is introduced to represent the real part of the  $q$ - $f$  correlator that is not determined by the response coefficient  $\lambda$ .

The role of detector in a quantum measurement is to convert the quantum input signal, in our case, the oscillations  $x(t) = x_0\sigma_z(t)/2$ , into the output signal that is already classical and can be dealt with (e.g., monitored or recorded) without “fundamental” problems. Condition of the classical behavior of the detector output requires the output spectral density to be much larger than the spectral density of the zero-point fluctuations in the relevant range of low frequencies of the input signal. For a detector with a short internal time scale this means that the noise  $q(t)$  is  $\delta$ -correlated on the time scale of the input signal:

$$\langle q(t+\tau)q(t) \rangle_0 = 2\pi S_q \delta(\tau). \quad (5)$$

Here  $S_q$  is the constant low-frequency part of the spectral density  $S_q(\omega)$  of the detector output noise.

For a quantum-limited detector at small temperature  $T \rightarrow 0$ , eqs. (4) and (5) impose a constraint on the spectral density  $S_f$  of the coupling operator  $f$ . Indeed, eqs. (4) and (5) can be written explicitly in the basis of the energy eigenstates  $|k\rangle$  of the detector and give the following expression for the spectral density  $S_q$ :

$$S_q = \int d\varepsilon_k d\varepsilon_{k'} \nu(\varepsilon_k) \nu(\varepsilon_{k'}) \rho_k \langle k|q|k' \rangle \langle k'|q|k \rangle \delta(\varepsilon_k - \varepsilon'_{k'} - \omega). \quad (6)$$

Expression for the correlation amplitude  $S_{qf}$  is similar, with the matrix element  $\langle k'|q|k \rangle$  replaced by the matrix element of  $f$ . In these expressions,  $\varepsilon_k$  is the energy of the state  $|k\rangle$ ,  $\rho_k$  is the probability to be in this state, and  $\nu$  is the state energy density. Since  $S_q$  is independent of the frequency  $\omega$ , eq. (6) is satisfied when the matrix elements of  $q$  and the density of states are constant, and eq. (6) can then be written as

$$S_q = |\langle q \rangle|^2 \nu^2.$$

It should be noted that the constant matrix elements  $\langle q \rangle$  and  $\langle f \rangle$  are off-diagonal in the  $k$ -basis and can be imaginary. Following the same steps for  $S_f$  we express this spectral density in terms of  $S_q$  and  $S_{qf}$ :

$$S_f = |\langle f \rangle|^2 \nu^2 = |S_{qf}|^2 / S_q. \quad (7)$$

Equations (7) and (4) relate the backaction noise of the detector determined by the spectral density  $S_f$  to its response coefficient and the output noise. Conceptually, such a relation resembles the fluctuation-dissipation theorem that links response of the system to its equilibrium fluctuations, but it does not have the status of a “theorem”. It is obvious from the derivation above that eq. (7) is not necessarily valid for an arbitrary system playing the role of detector in a quantum measurement.

Nevertheless, it holds for several of the “standard” detectors: quantum point contact, resistively-shunted dc SQUID, and Cooper-pair electrometer, considered later in this work.

Making use of  $q$ - and  $f$ -correlators, we can calculate the spectral density of the detector output  $o(t)$  in the process of continuous measurement of the MQC oscillations. From eq. (2), the correlation function of  $o(t)$  is:

$$K_o(\tau) = 2\pi S_q \delta(\tau) + \frac{\lambda^2}{4} \text{Tr}\{\rho \sigma_z \sigma_z(\tau)\}, \quad (8)$$

where  $\rho$  is the stationary density matrix of the two-state system established as a result of the interaction with the detector. Averaging the Heisenberg equation of motion of the operator  $\sigma_z(\tau)$  over the  $\delta$ -correlated backaction noise  $f$  of the detector, we get the set of equations for the time evolution of the matrix elements  $\sigma_{ij}$  of  $\sigma_z(\tau)$ :

$$\dot{\sigma}_{11} = \Delta \text{Im} \sigma_{12}, \quad \dot{\sigma}_{12} = (i\varepsilon - \Gamma) \sigma_{12} - i\Delta \sigma_{11}, \quad (9)$$

and  $\sigma_{22} = -\sigma_{11}$ , with the rate

$$\Gamma = \pi S_f \quad (10)$$

describing the backaction dephasing of the oscillations by the detector. The density matrix  $\rho$  of the two-state system satisfies the same set of equations (9), except for the normalization,  $\rho_{11} + \rho_{22} = 1$ , and its stationary value is  $\rho = 1/2$ . Solving eqs. (9) with the initial condition  $\sigma_z(0) = \sigma_z$  and averaging  $\sigma_z \sigma_z(\tau)$  over  $\rho = 1/2$  we find the spectral density  $S_o(\omega) = (1/2\pi) \int_{-\infty}^{\infty} K_o(\tau) e^{i\omega\tau} d\tau$ . Under the conditions of “resonance”,  $\varepsilon = 0$ , when the oscillation amplitude is maximum, we get:

$$S_o(\omega) = S_q + \frac{\Gamma \lambda^2}{4\pi} \frac{\Delta^2}{(\omega^2 - \Delta^2)^2 + \Gamma^2 \omega^2}. \quad (11)$$

When  $\varepsilon \neq 0$ , it is convenient to calculate the spectrum numerically from eq. (9). The spectrum in this case is plotted in Fig. 2 for several values of  $\varepsilon$  and the dephasing rate  $\Gamma$ . For weak dephasing,  $\Gamma \ll \Delta$ , the spectrum consists of a zero-frequency Lorentzian that vanishes at  $\varepsilon = 0$  and grows with increasing  $|\varepsilon|$ , and a peak at the oscillation frequency  $\Omega = (\Delta^2 + \varepsilon^2)^{1/2}$ . The peak at zero frequency reflects the incoherent transitions with a small rate of order  $\Gamma$  between the states of the two-state system. The high-frequency peak of the MQC oscillations also has the width  $\Gamma$ . While this width can be small for sufficiently weak dot-contact coupling, the height of the oscillation peak cannot be arbitrarily large in comparison to the background noise spectral density  $S_q$ . At  $\varepsilon = 0$ , when the amplitude of the oscillations is maximum, the peak height is  $S_{max} = \lambda^2 / 4\pi\Gamma$ . Even in this case, the ratio of the peak height to the background is limited:

$$\frac{S_{max}}{S_q} = \frac{\lambda^2}{4\pi^2 S_f S_q} = \frac{4\lambda^2}{\lambda^2 + a^2} \leq 4. \quad (12)$$

This limitation is universal, e.g., independent of the coupling strength between the detector and oscillations,

and reflects quantitatively the interplay between measurement of the MQC oscillations and their backaction dephasing. The fact that the height of the spectral line of the oscillations can not be much larger than the noise background means that, in the time domain, the oscillations are drowned in the shot noise.

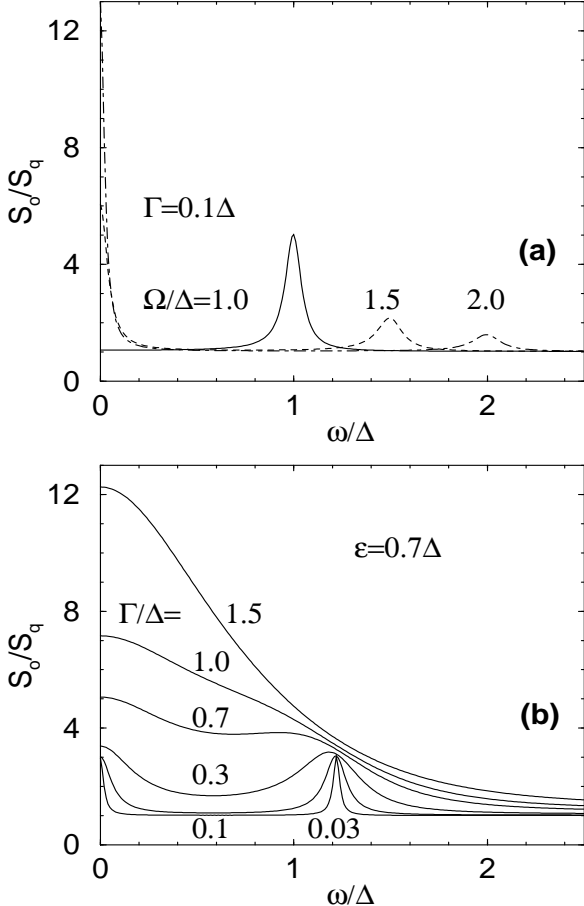


FIG. 2. Spectral density  $S_o(\omega)$  of the output of the symmetric detector with minimal backaction dephasing ( $a = 0$ ) measuring the MQC oscillations for several values of (a) the energy bias  $\varepsilon$  reflected in the oscillation frequency  $\Omega = (\Delta^2 + \varepsilon^2)^{1/2}$ , and (b) the rate  $\Gamma$  (10) of the measurement-induced dephasing.

When the backaction dephasing rate  $\Gamma$  increases, the oscillation line broadens towards the lower frequencies, and eventually turns into the growing spectral peak at zero frequency associated with the incoherent jumps between the two basis states of the two-state system. At large  $\Gamma$ , when the coherent oscillations are suppressed, the rate of incoherent tunneling decreases with increasing  $\Gamma$ . For instance, at  $\Gamma \gg \Omega$ , the tunneling rate is  $\gamma = \Delta^2/2\Gamma$ , and the spectral density of the detector response at low frequencies  $\omega \sim \gamma$  has the standard Lorentzian form,  $S_o(\omega) - S_q = 2\gamma\lambda^2/4\pi(4\gamma^2 + \omega^2)$ . Suppression of the tunneling rate  $\gamma$  with increasing dephasing rate  $\Gamma$  is an example of the generic ‘‘Quantum Zeno Effect’’ in which quantum measurement suppresses the

decay rate of a metastable state. In the context of search for the macroscopic quantum coherent oscillations, the Lorentzian spectral density has been observed and used for measuring the tunneling rate of incoherent quantum flux tunneling in SQUIDs<sup>26</sup>.

The maximum signal-to-noise ratio  $S_{max}/S_q$  (12) is attained if the fundamental backaction of the detector is the only mechanism of dephasing of the coherent oscillations. We now discuss briefly the effect of a weak additional dephasing and energy-relaxation on the spectral density of the oscillations. The effect of such a weak relaxation is noticeable if the backaction dephasing is also weak,  $\Gamma \ll \Delta$ . Energy relaxation arises typically due to interaction with some external system (‘‘reservoir’’) that is in equilibrium at temperature  $T$ . The interaction term in the Hamiltonian can be written similarly to the interaction with the detector (1) as

$$H_c = -\sigma_z f_r, \quad (13)$$

where  $f_r$  is the reservoir force acting on the system. Under the assumption of the frequency-independent relaxation rate, the standard free equilibrium correlator of this force is (see, e.g.,<sup>27</sup>):

$$\langle f_r(t) f_r(t + \tau) \rangle = \alpha \int \frac{d\omega}{\pi} \frac{\omega e^{i\omega\tau}}{1 - e^{-\omega/T}}, \quad (14)$$

where parameter  $\alpha$  characterizes the relaxation strength. Comparison of this correlator with the  $\delta$ -correlated backaction noise of the detector shows that the detector (1) is acting effectively as a reservoir with temperature that is much larger than the energies of the two-state system.

Energy relaxation makes the stationary average value of  $\sigma_z$  non-vanishing, and the output correlation function should now be calculated as

$$K_o(\tau) = K_q(\tau) + \frac{\lambda^2}{8} [\langle \sigma_z \sigma_z(\tau) + \sigma_z(\tau) \sigma_z \rangle - 2\langle \sigma_z \rangle^2]. \quad (15)$$

For weak coupling, it is convenient to find the time evolution of  $\sigma_z(\tau)$  in the basis of eigenstates of the two-state Hamiltonian. In this basis, the Hamiltonian including interaction with the reservoir (and omitting temporarily the detector) is :

$$H = -\frac{1}{2}\Omega\sigma_z - \frac{1}{\Omega}(\varepsilon\sigma_z - \Delta\sigma_x)f_r + H_r. \quad (16)$$

$H_r$  is the Hamiltonian of the reservoir. Heisenberg equations of motion that follow from the Hamiltonian (16) are:

$$\dot{f}_r = i[H_r, f_r], \quad \dot{H}_r = \frac{i}{\Omega}(\Delta\sigma_x - \varepsilon\sigma_z)[f_r, H_r],$$

$$\dot{\sigma}_z = 2f_r\Delta\sigma_y, \quad \dot{\sigma}_{\pm} = \mp i(\Omega + 2\varepsilon f_r/\Omega)\sigma_{\pm} \mp i\Delta\sigma_z/\Omega,$$

where  $\sigma_{\pm} \equiv (\sigma_x \pm i\sigma_y)/2$ . Integration of the first two of these equations gives in the first order in coupling (13) to the two-state system:

$$f_r(t) = f_r^{(0)}(t) - i\Delta \int^t d\tau \int^\tau d\tau' [f_r^{(0)}(\tau), f_r^{(0)}(\tau')] \sigma_y(\tau'),$$

where  $f_r^{(0)}$  is the free part of the fluctuating reservoir force in absence of coupling. Solving the second pair of the Heisenberg equations up to the second order in coupling, making the rotating-wave approximation, and tracing out the reservoir degrees of freedom with the help of the correlator (14), we get a set of equations for the evolution of the matrix elements  $s_{ij}$  of the operator of the oscillating variable (given by  $\sigma_z(\tau)$  in the original “position” basis) in the eigenstate basis:

$$\dot{s}_{jj}(\tau) = \Gamma_e \left[ \frac{\varepsilon}{\Omega} - \coth \left\{ \frac{\Omega}{2T} \right\} s_{jj} \right] + (-1)^j \frac{\Gamma \Delta^2}{2\Omega^2} (s_{11} - s_{22}),$$

$$\dot{s}_{12}(\tau) = (i\varepsilon - \Gamma_0) s_{12}. \quad (17)$$

Initial conditions for these equations are:  $s_{11} = -s_{22} = \varepsilon/\Omega$ , and  $s_{12} = -\Delta/\Omega$ . The characteristic energy-relaxation rate in eq. (17) is  $\Gamma_e = 2\alpha\Delta^2/\Omega$ , and the total dephasing rate is

$$\Gamma_0 = \frac{1}{\Omega^2} \left[ \alpha(\Delta^2 \Omega \coth \left\{ \frac{\Omega}{2T} \right\} + 4\varepsilon^2 T) + \Gamma(\varepsilon^2 + \frac{\Delta^2}{2}) \right].$$

In eqs. (17), we also added the detector dephasing terms from eq. (9) “rotated” from the position basis into the eigenstate basis.

The density matrix  $r$  of the two-state system in the basis of eigenstates satisfies similar equations, and the stationary values of its matrix elements are  $r_{12} = 0$  and  $r_{11} = (\Gamma_t + \Gamma_e)/2\Gamma_t$ , where

$$\Gamma_t \equiv \Gamma_e \coth(\Omega/2T) + \Gamma \Delta^2 / \Omega^2.$$

Using these relations, the definition (15), and the evolution equations (17) we find the spectral density:

$$S_o(\omega) = S_q + \frac{\lambda^2}{4\pi\Omega^2} \times \left( [1 - (\frac{\Gamma_e}{\Gamma_t})^2] \frac{2\varepsilon^2 \Gamma_t}{\omega^2 + \Gamma_t^2} + \sum_{\pm} \frac{\Delta^2 \Gamma_0}{(\omega \pm \Omega)^2 + \Gamma_0^2} \right). \quad (18)$$

As in the case without energy relaxation, the spectral density consists of a zero-frequency Lorentzian of width  $\Gamma_t$  and peaks at  $\pm\Omega$  of width  $\Gamma_0$  due to coherent oscillations. For weak relaxation, the incoherent slow transitions giving rise to the low-frequency noise are the transitions between the two energy eigenstates of the system. The height of the oscillation peak is suppressed in presence of additional energy relaxation that contributes to the dephasing rate  $\Gamma_e$ , and the relative magnitude of the peak,  $S_{max}/S_q$  is smaller than its value without the relaxation.

### III. RELATION TO ENERGY SENSITIVITY

The detector characteristics for measurement of the quantum coherent oscillations in a two-state system considered in the previous Section are related to another detector characteristic that is used for measurements of the harmonic signals – see, e.g., examples in<sup>28–31</sup>, and sometimes is loosely referred to as “energy sensitivity”. It is defined by considering the detector measuring a harmonic oscillator with a frequency  $\omega_0$  and a small relaxation rate  $\gamma \ll \omega_0$ . In this Section, we establish the quantitative relation between the signal-to-noise ratio  $S_{max}/S_q$  for measurements of the two-state systems discussed above with the energy sensitivity used in the literature for measurements of harmonic signals.

The Hamiltonian of the damped harmonic oscillator attached to a detector is obtained by replacing the two-state part of eqs. (1) and (13) with the corresponding oscillator terms:

$$H = \frac{M}{2}(\dot{x}^2 + \omega_0^2 x^2) - x(f + f_r) + H_0 + H_r, \quad (19)$$

where  $M$  is the mass of the oscillator and  $x$  is the oscillating coordinate. Due to linearity of the system, the Heisenberg equation of motion for  $x$  that follow from the Hamiltonian (19) (see, e.g.,<sup>27</sup>) coincides with the classical equation of motion of the damped oscillator:

$$\ddot{x} - \gamma \dot{x} + \omega_0^2 x = \frac{1}{M}(f_r(t) + f(t)). \quad (20)$$

As in the previous Section, the random forces  $f_r(t)$  and  $f(t)$  are produced, respectively, by the reservoir responsible for the energy relaxation of the oscillator and by the detector. (Although the operators  $f_r$  and  $f$  in eqs. (19) and (20), as well as the transfer coefficient  $\lambda$  in eq. (21) below, differ from the corresponding quantities used in Section 2 by a normalization factor, this distinction is not made explicit. This should not lead to any confusion, since the normalization factor drops out of all expression which are compared between the two Sections.) In general, the right-hand-side of eq. (20) should also contain an external perturbation that creates a “signal” component of the oscillations  $x(t)$ . However, for the discussion of the detector sensitivity, it is appropriate to treat the equilibrium fluctuations of the oscillator driven by the reservoir noise  $f_r(t)$  (e.g., the zero-point oscillations at vanishing temperature  $T$ ) as part of the signal. This allows us not to include additional signal terms in eq. (20).

The sensitivity of the detector is characterized by the detector noise contribution to the spectral density of the output  $S_o$  reduced to the detector input. Similarly to eq. (2) the output of the detector measuring harmonic oscillator is:

$$o(t) = q(t) + \lambda x(t). \quad (21)$$

This equation implies that the detector contribution to the output noise comes from the two sources: direct output noise  $q(t)$ , and effect of the backaction noise  $f(t)$  on

the oscillator coordinate  $x(t)$ . Introducing the dynamic response function  $G(t)$  of the oscillator:

$$x(t) = \int_0^{+\infty} d\tau G(\tau) (f_r(t-\tau) + f(t-\tau)), \quad (22)$$

with  $G(\tau) = 0$  for  $\tau < 0$ , we see from eq. (20) that

$$G(\omega) = \int d\tau e^{-i\omega\tau} G(\tau) = \frac{1}{M} \frac{1}{\omega_0^2 - \omega^2 + i\gamma\omega}. \quad (23)$$

In terms of the response function,  $x(\omega) = G(\omega)(f_r(\omega) + f(\omega))$ .

Since the detector noise  $f(t)$  is uncorrelated with the reservoir force  $f_r(t)$ , or in general, any other signal component of  $x(t)$ , we see from eqs. (21), (22), and (23) that the spectral density of the detector output consists of the two additive components: signal, i.e., equilibrium spectral density of the harmonic oscillations transformed to the output, and the detector noise  $S_N(\omega)$ :

$$S_o(\omega) = \lambda^2 |G(\omega)|^2 S_r(\omega) + S_N(\omega),$$

$$S_N(\omega) = S_q + \lambda^2 |G(\omega)|^2 S_f + 2\lambda \text{Re}G(\omega) \bar{S}_{qf}. \quad (24)$$

Here  $\bar{S}_{qf}$  is the symmetrized correlator of the detector output and input noises,  $\bar{S}_{qf} = (S_{qf} + S_{fq})/2 = a/4\pi$  (with  $a$  defined in eq. (4)), and  $S_r(\omega)$  is the spectral density of the reservoir force  $f_r$ :

$$S_r(\omega) = (\gamma\omega M/2\pi) \coth(\hbar\omega/2T). \quad (25)$$

The noise properties of the detector are better characterized if its contribution to the output noise is reduced to the input, i.e. instead of  $S_N(\omega)$  (24) we consider the quantity  $F(\omega) \equiv S_N(\omega)/\lambda^2 |G(\omega)|^2$ . For weak damping,  $\gamma \ll \omega_0$ , when

$$|G(\omega)|^2 \simeq \frac{1}{4\omega_0^2 M^2 ((\omega - \omega_0)^2 + \gamma^2/4)},$$

we get

$$F(\omega) = S_f + S_q (2\omega_0 M/\lambda)^2 ((\omega - \omega_0)^2 + \gamma^2/4) - \bar{S}_{qf} (4\omega_0 M/\lambda) (\omega - \omega_0).$$

The three terms in this equation scale differently with the strength of the detector-oscillator coupling, since  $\lambda$  and  $\bar{S}_{qf}$  are proportional to the first power, while  $S_f$  is proportional to the second power of the coupling strength.  $F(\omega)$  can be minimized with respect to the coupling strength and also with respect to the small detuning  $\omega - \omega_0$  between the signal frequency and the oscillator frequency. The minimum is reached when

$$\omega - \omega_0 = \frac{\lambda \bar{S}_{qf}}{2\omega_0 M S_q},$$

and

$$\lambda = \frac{\gamma\omega_0 M S_q}{S_0}, \quad S_0 \equiv (S_q S_f - \bar{S}_{qf}^2)^{1/2},$$

and is equal to

$$F_{min} = 2\gamma\omega_0 M \frac{S_0}{\lambda}. \quad (26)$$

It is convenient to normalize the reduced noise  $F$  in such a way that it can be directly compared to the equilibrium fluctuations in the oscillator driven by  $S_r$ . Since at this stage we can already neglect small difference between the oscillator frequency and signal frequency, both the minimum noise  $F_{min}$  (26) and the equilibrium spectral density  $S_r$  (25) are proportional to the oscillator parameters  $\gamma\omega_0 M$ . This means that with appropriate normalization we can define  $F_{min}$  directly in terms of the number of quanta added to the signal at frequency  $\omega$  by the detector. This is achieved by introducing the energy sensitivity as

$$\epsilon \equiv \frac{\pi}{\gamma\omega_0 M} F_{min} = \frac{2\pi}{\lambda} (S_q S_f - \bar{S}_{qf}^2)^{1/2}. \quad (27)$$

Equations (7) and (4) of the previous Section show that for a quantum-limited detector

$$\epsilon = \hbar/2. \quad (28)$$

(Note that in this Chapter,  $\hbar$  is shown only in some of the final results.) Equation (28) agrees with the conclusion of a general theory of quantum linear amplifiers, according to which a phase-insensitive linear amplifier adds at least half-a-quantum of noise to the amplified signal – see, e.g.,<sup>32</sup>. This result is related to eq. (ref39) since detector in the measurement process plays the role of an amplifier transforming weak quantum input signal into the classical output.

Comparing eq. (27) for the energy sensitivity with eq. (12) for the signal-to-noise ratio of the measurement of the quantum coherent oscillations we see finally that these two quantities are closely related. When the output and input noises of the detector are uncorrelated,  $S_{qf} = 0$ , the relation is simple:

$$\frac{S_{max}}{S_q} = (\hbar/\epsilon)^2. \quad (29)$$

As will be clear from the examples of specific detector considered below, the situation with  $\bar{S}_{qf} = 0$  can be reasonably referred to as “symmetric detector”. As follows from eq. (ref40), the largest signal-to-noise ratio of 4 is obtained for such a symmetric detector in the quantum-limited regime with  $\epsilon = \hbar/2$ .

When the input-output correlation is non-vanishing, the signal-to-noise ratio is smaller than the value given by eq. (29), while the energy sensitivity  $\epsilon$  for measurement of the harmonic signal can still be made equal to

$\hbar/2$  by optimizing the detuning between the signal and the oscillator. Another difference between the measurement of harmonic oscillator defining  $\epsilon$  and measurement of the two-state system, is that the minimum noise (26) in the oscillator measurement is reached only for optimum detector-oscillator coupling, while the maximum signal-to-noise ratio (12) for the quantum oscillation measurement is independent of the coupling strength to the detector as long as the coupling is weak.

#### IV. ENERGY SENSITIVITY OF A QUANTUM POINT CONTACT

One of the applications of the results obtained in the previous Section is the demonstration that a quantum point contact that is frequently used as the detector of electric charge or voltage<sup>33–36</sup> can reach the quantum-limited regime with ultimate energy sensitivity (28). The mechanism of operation of a quantum point contact as a detector utilizes modifications of the electron transmission properties of the contact by the measured voltage<sup>33</sup>. When the contact is biased with a large voltage  $V$ , changes in the electron transmission probability lead to changes in the current  $I$  flowing through the contact which serve as the measurement output. Fluctuations of the electric potential in the contact region due to the current flow produce the backaction dephasing of the measured object by the point contact<sup>35,36</sup>. This dephasing was calculated for symmetric contacts within different approaches in<sup>37–41</sup>. It is known<sup>42,25</sup> that in the case of measurement of a two-state system, when the coupling to the system is symmetric, quantum point contact is an ideal detector of the quantum coherent oscillations. Such a detector causes the minimum dephasing of the oscillations that is consistent with the information acquisition by the measurement. For asymmetric coupling, the dephasing by the point contact is larger than the fundamental minimum<sup>25,36</sup>.

To calculate the energy sensitivity of the point contact detector, we start with the standard Hamiltonian of a single-mode point contact. Including a weak additional scattering potential  $U(x)$  for the point contact electrons which is the input signal of the measurement we can write the Hamiltonian as

$$H = \sum_{ik} \epsilon_k a_{ik}^\dagger a_{ik} + U, \quad U = \sum_{ij} U_{ij} \sum_{kp} a_{ik}^\dagger a_{jp}. \quad (30)$$

The operators  $a_{ik}$  in this Hamiltonian represent point-contact electrons in the two scattering states  $i = 1, 2$  (incident from the two contact electrodes) with momentum  $k$ , and  $U_{ij} = \int dx \psi_i^*(x) U(x) \psi_j(x)$  are the matrix elements of the potential  $U(x)$  in the basis of the scattering states. Here  $\psi_i(x)$  is the wavefunction of the scattering state, and  $x$  is the coordinate along the point contact. Several assumptions are made about the contact. The

bias energy  $eV$  is assumed to be much larger than temperature  $T$ , but much smaller than both the Fermi energy in the point contact and the inverse traversal time of the contact. This allows us to linearize the energy spectrum of the point-contact electrons:  $\epsilon_k = v_F k$ , where  $v_F$  is the Fermi velocity, and neglect the momentum dependence of the matrix elements  $U_{ij}$ . The potential  $U(x)$  is also assumed to be sufficiently weak and can be treated as perturbation. In this regime, the point contact operates as a linear detector, and the current response to the perturbation  $U$  can be calculated in the linear-response approximation. The last assumption is that the frequencies of the input signal are much smaller than  $eV$ , the fact that allows to treat  $U$  as the static perturbation.

At frequencies much lower than both  $eV$  and inverse traversal time of the contact, the current is constant throughout the contact and the contact response can be calculated at any point  $x$ . We choose the origin of the coordinate  $x$  in such a way that the unperturbed scattering potential is effectively symmetric, i.e., the reflection amplitudes for both scattering states are the same, and then take  $x$  to lie in the asymptotic region of the scattering states. In this case, the standard expression for the current in terms of the electron operators  $\Psi(x)$ :

$$I = \frac{-ie\hbar}{2m} (\Psi^\dagger \frac{\partial \Psi}{\partial x} - \frac{\partial \Psi^\dagger}{\partial x} \Psi), \quad \Psi(x) = \sum_{ik} \psi_{ik}(x) a_{ik},$$

gives for the current operator at  $x$ :

$$I = \frac{ev_F}{L} \sum_{kp} [D(a_{1k}^\dagger a_{1p} - a_{2k}^\dagger a_{2p}) + i(DR)^{1/2} e^{-i(k-p)|x|} (a_{1k}^\dagger a_{2p} - a_{2k}^\dagger a_{1p})]. \quad (31)$$

Here  $D$  and  $R = 1 - D$  are the transmission and reflection probabilities of the point contact,  $L$  is a normalization length, and the variation of the momentum near the Fermi points (i.e., the difference between  $k$  and  $p$ ) was neglected everywhere besides the phase factor in the second term. The reason for keeping this factor will become clear later.

In the linear-response regime, the current response of the point contact is driven by the part of the perturbation  $U$  causing transitions between the two scattering states  $\psi_{1,2}$ . As shown in the Appendix, the real part of the transition matrix element  $U_{12}$  is related to the change  $\delta D$  of the transmission probability of the contact:

$$U_{12} = \frac{v_F}{L} \frac{\delta D + iu}{2(DR)^{1/2}}, \quad U_{21} = U_{12}^*. \quad (32)$$

The imaginary part of  $U_{12}$ , expressed through a dimensionless parameter  $u$  in eq. (4), does not affect the current  $I$ . Qualitatively, it characterizes the degree of asymmetry in the coupling of the quantum dots to the point contact;  $u = 0$  if the perturbation potential  $U(x)$  is applied symmetrically with respect to the main scattering potential of the point contact.

In the measurement process, the perturbation  $U$  represents the coupling operator between the contact and the measured system, whereas the current  $I$  is the measurement output. As follows from the discussion in the previous Section, the energy sensitivity of the contact is determined by the correlators of  $U$  and  $I$ , and by the response coefficient  $\lambda$ . Using eqs. (30), (31), and (32) we can evaluate the correlators directly. In the limit of large voltages,  $eV \gg T$ , when the contact noise properties are dominated by the shot noise, we get:

$$\begin{aligned}\langle U(t)U(t+\tau) \rangle_0 &= \frac{eV}{4\pi} \frac{(\delta D)^2 + u^2}{DR} \delta(\tau), \\ \langle I(t+\tau)I(t) \rangle_0 &= \frac{e^3 V D R}{\pi} \delta(\tau), \\ \langle U(t)I(t+\tau) \rangle_0 &= \frac{e^2 V}{2\pi} (i\delta D + u) \delta(\tau - \eta).\end{aligned}\quad (33)$$

The time delay  $\eta \equiv |x|/v_F$  in the last of eqs. (33) comes from the phase factor  $e^{-i(k-p)|x|}$  kept in eq. (31), and is infinitesimally small for small traversal time of the contact. It is nevertheless important for correct calculation of the contact response  $\lambda$ . From the  $U$ - $I$  correlator and the standard expression for the linear response (3) we confirm that  $\lambda$  is equal to the change of current through the contact due to change  $\delta D$  of the transmission coefficient,  $\lambda = e^2 V \delta D / \pi$ .

The correlators (33) satisfy the general relations (7) and (4), and therefore the energy sensitivity of the quantum point contact reaches the fundamental quantum limit (28). It should be noted, however, that this conclusion is strictly valid only in the large-voltage limit  $eV \gg T$ . At finite temperature  $T$ , scattering of the point-contact electrons within the same direction of propagation (described by the terms  $U_{11}$  and  $U_{22}$  of the perturbation  $U$ ) creates additional contribution to the back-action noise and degrades the energy sensitivity. The magnitude of this effect depends on the magnitude of the “forward” scattering matrix elements  $U_{11}$  and  $U_{22}$  relative to the backscattering matrix element  $U_{12}$ , increasing with intensity of the forward scattering but decreasing with  $T/eV$  ratio.

## V. FLUX AND CHARGE MQC OSCILLATIONS

This Section provides specific examples of measurements of the macroscopic quantum coherent oscillations of magnetic flux and electric charge. It is shown that the typical detectors for the flux and charge measurements, dc SQUID and Cooper-pair electrometer, satisfy the general equations of Sections 2 and 3, and should be capable of reaching the fundamental limit of the signal-to-noise ratio for the continuous weak measurement of the MQC oscillations.

### A. Flux oscillations measured with a dc SQUID

Typical set-up of a measurement of the MQC oscillations of flux with a dc SQUID consists of a two-state flux system (rf SQUID with half of a magnetic flux quantum  $\Phi_0 = \pi\hbar/e$  induced in it by an external magnetic field) coupled inductively to a dc SQUID biased with an external current  $I_0$  and shunted by a resistor  $R$  (Fig. 3). When the inductance of dc SQUID loop is small, the difference between the two Josephson phases  $\varphi_{1,2}$  across the two junctions of the SQUID is directly linked to the flux  $\Phi$  induced in the dc SQUID by the flux oscillations:

$$\varphi_1 - \varphi_2 = 2\pi\Phi/\Phi_0 \equiv \Theta.$$

In this case, the SQUID is equivalent to a single Josephson junction, with the supercurrent in this junction modulated by the flux  $\Phi$ . The total amplitude of Cooper-pair tunneling in the SQUID is equal to a sum of the two individual amplitudes of tunneling in the two SQUID junction, and can be written as

$$E_J/2 = I^{(+)}(\Theta)/4e, \quad I^{(+)}(\Theta) = I_1 e^{i\Theta/2} + I_2 e^{-i\Theta/2}, \quad (34)$$

where  $I_{1,2}$  are the critical currents of the two junctions. Coherent sum of the two tunneling amplitudes in (34) leads to modulation of the total supercurrent of the SQUID.

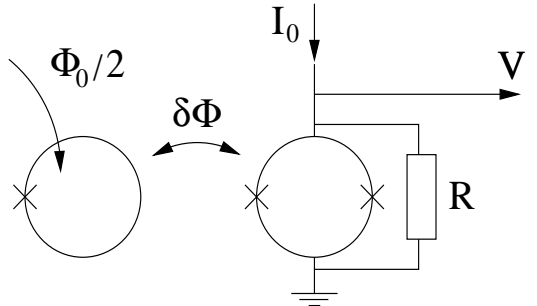


FIG. 3. Schematic diagram of a continuous measurement of the MQC oscillations of magnetic flux with a dc SQUID. The two-state flux system is implemented as an rf SQUID with externally induced flux  $\Phi_0/2$  and is coupled to the dc SQUID biased with a current  $I_0$ . The coupling strength is characterized by the variation  $\delta\Phi$  of the flux through the dc SQUID due to oscillations. The voltage  $V$  across the dc SQUID is the measurement output.

We consider the simplest regime of the dc SQUID dynamics when the bias current  $I_0$  and associated average voltage  $V_0 = RI_0$  across the dc SQUID are sufficiently large, and the dc component of the Josephson current through it is small in comparison to  $I_0$ . In this regime, the Cooper-pair tunneling through the SQUID is adequately described by perturbation theory in the tunneling amplitude (34) and can be qualitatively interpreted

as incoherent jumps of individual Cooper pairs. The resistor  $R$  provides the dissipation mechanism that transforms reversible dissipationless Cooper-pair oscillations between the two electrodes of the SQUID into incoherent tunneling.

Using the known results for the incoherent Cooper-pair tunneling<sup>43</sup>, we can calculate the rate of this tunneling and find all the detector characteristics of the dc SQUID. The SQUID is coupled to the oscillations by the operator of the current  $I_-$  circulating in the SQUID loop multiplied by the change  $\delta\Phi$  of the flux in the loop induced by the flux oscillations. Changes in the flux through the dc SQUID change the total current  $I_+$  through both SQUID junctions and create deviations  $V$  of the voltage across the SQUID from  $V_0$ ,  $V = -RI_+$ , that serve as the measurement output. As follows from the general discussion in Sec. 2, SQUID parameters important for measurement are the coefficient  $\lambda$  of the transformation of the oscillating flux into the voltage  $V$ , the spectral density  $S_I$  of the circulating current  $I_-$  that is responsible for back-action dephasing by the SQUID, the spectral density of the output voltage  $S_V$ , and the correlator  $S_{VI}$  between  $V$  and  $I_-$ . These parameters can be found quantitatively starting from the tunneling part  $H_T$  of the SQUID Hamiltonian that can be written as

$$H_T = -\frac{E_J}{2}e^{i(2eV_0t+\varphi(t))} + h.c., \quad (35)$$

with  $\varphi(t)$  being the random Josephson phase across the dc SQUID accumulated due to equilibrium voltage fluctuations produced by the resistor  $R$ . It is characterized by the correlator

$$\langle\varphi(t)\varphi\rangle = \rho \int \frac{d\omega}{\omega} g(\omega) \frac{e^{i\omega t}}{1 - e^{-\omega/T}}, \quad (36)$$

where  $\rho = R/R_Q$  is the resistance  $R$  in units of the quantum resistance  $R_Q = \pi\hbar/4e^2$ , the average  $\langle \dots \rangle$  is taken over equilibrium density matrix of the resistor  $R$ , and  $g(\omega)$  describes the cut-off of the dissipation provided by  $R$  at some large frequency  $\omega_c$  associated with either finite inductance of the SQUID or finite capacitance of its junctions, while  $g(\omega) = 1$  at  $\omega \ll \omega_c$ .

The operators of the two currents  $I_\pm$  that determine the SQUID parameters are:

$$I_\pm = \frac{-i}{2}[I^{(\pm)}(\Theta)e^{i(2eV_0t+\varphi(t))} - h.c.], \quad (37)$$

$$I^{(-)} \equiv (I_1 e^{i\Theta/2} - I_2 e^{-i\Theta/2})/2.$$

In the regime of the incoherent Cooper-pair tunneling the average dc current  $\langle I_+ \rangle$  can be found treating the tunneling  $H_T$  as perturbation:

$$\langle I_+ \rangle = -i \int_0^\infty dt \langle [I_+, H_T(t)] \rangle = \pi |I^{(+)}(\Theta)|^2 \tau / e, \quad (38)$$

where

$$\tau \equiv \frac{1}{4\pi} \text{Re} \int_0^\infty dt e^{i2eV_0t} \langle [e^{i\varphi(t)}, e^{-i\varphi}] \rangle. \quad (39)$$

For example, for vanishing temperature  $T$ , and small bias voltages,  $2eV_0 \ll \omega_c$ , the time  $\tau$  defined in (39) can be found from eqs. (39) and (36) to be (see, e.g.,<sup>44</sup>):

$$\tau = (1/4\omega_c \Gamma(\rho)) (2eV_0/\omega_c)^{\rho-1}. \quad (40)$$

When the resistance  $R$  is small,  $R \ll R_Q$ ,  $\tau$  becomes independent of  $\omega_c$ ,  $\tau = eR/2\pi V$ . In this case, all the SQUID characteristics, including the average current  $\langle I_+ \rangle$  (38) can be obtained by direct time averaging of the classical Josephson oscillations in the SQUID.

The noise spectral densities of the two currents,  $I_\pm$ , are obtained by directly taking the average over equilibrium density matrix of the resistor  $R$ . They vary with frequency on the scale of the Josephson frequency  $2eV_0$ , and are constant at  $\omega \ll 2eV_0$ . In this frequency range,

$$S_I = \frac{1}{2\pi} \int dt \langle I_-(t) I_- \rangle = \frac{1}{8\pi} |I^{(-)}(\Theta)|^2 \times \\ \int dt e^{i2eV_0t} \langle [e^{i\varphi(t)}, e^{-i\varphi}]_+ \rangle. \quad (41)$$

Fluctuation-dissipation theorem relates the anticommutator  $[\dots]_+$  in this equation to the commutator in eq. (39) and gives:

$$S_I = |I^{(-)}(\Theta)|^2 \tau', \quad S_V = R^2 |I^{(+)}(\Theta)|^2 \tau', \quad (42)$$

where  $\tau' \equiv \tau \coth(eV_0/T)$ . The correlation function  $S_{VI}$  is found similarly:

$$S_{VI} = R [I^{(+)}(\Theta)]^* I^{(-)}(\Theta) \tau'. \quad (43)$$

Comparison of the spectral density  $S_V$  (42) and the average current (38) shows that  $S_{I+} = S_V/R^2 = (e\langle I_+ \rangle/\pi) \coth(eV_0/T)$ , i.e. the noise of the current  $I_+$  can indeed be interpreted as resulting from uncorrelated transitions of individual Cooper pairs. In particular, at  $T \ll eV_0$ , the noise is the shot noise of Cooper pairs.

Finally, eq. (38) gives the response coefficient of the SQUID

$$\lambda \equiv \partial V / \partial \Phi = 2\pi R (\partial |I^{(+)}(\Theta)|^2 / \partial \Theta) \tau. \quad (44)$$

(Note that as in eq. (42) for the backaction noise  $S_I$  and also in eq. (43) for the correlator  $S_{VI}$ , the factor  $\delta\Phi$  is omitted from the definition of  $\lambda$ .)

For temperatures negligible on the scale of  $eV_0$ ,  $\tau'$  in the noise spectral densities is equal to  $\tau$  and eqs. (42) through (44) show that the spectral densities  $S_V$ ,  $S_I$ , and  $S_{VI}$  satisfy the general relation (7), and since  $\partial |I^{(+)}(\Theta)|^2 / \partial \Theta = -2\text{Im}\{[I^{(+)}(\Theta)]^* I^{(-)}(\Theta)\}$ , the correlator  $S_{VI}$  is also related to the response coefficient  $\lambda$  by the expression identical to eq. (4). Moreover, since

$$[I^{(+)}(\Theta)]^* I^{(-)}(\Theta) = \frac{1}{2}(I_1^2 - I_2^2) + iI_1 I_2 \sin \Theta,$$

we see that the real part of the correlator  $S_{VI}$ , which increases backaction dephasing produced by the SQUID, is indeed associated with the SQUID asymmetry. When  $I_1 = I_2$ , the real part vanishes and the SQUID as detector reaches quantum-limited optimum for measurement of the quantum coherent oscillations. For such a symmetric SQUID the signal-to-noise ratio of the oscillation measurement is given by eq. (29) (with the intensity of background output noise given by  $S_V$ ). If the temperature  $T$  of the symmetric SQUID is negligible, eqs. (42) through (44), and (27) show that in this regime the SQUID is the quantum-limited detector with the energy sensitivity  $\epsilon = \hbar/2$ , and the signal-to-noise ratio for measurement of the quantum flux oscillations is  $S_{max}/S_V = 4$ . When  $T$  becomes non-vanishing, both the output and backaction noise increase,  $\tau' > \tau$ , and eq. (29) describes the gradual suppression of the signal-to-noise ratio with increasing temperature.

## B. Charge oscillations measured with a Cooper-pair electrometer

Coherent oscillations of charge take place in Josephson junctions which are sufficiently small for the charging energy  $E_C$  of an individual Cooper pair,  $E_C = (2e)^2/2C$  to be larger than temperature  $T$  and Josephson coupling energy  $E_J$ . The supercurrent flow through the junction is “discretized” in this regime into the transfer of individual Cooper pairs by strong Coulomb repulsion. Quantitatively, if the charging energy is smaller than the superconducting energy gap  $\Delta$  so that the dissipative quasiparticle tunneling is suppressed, the junction dynamics is governed by the simple Hamiltonian:

$$H = E_C(n - q)^2 - \frac{E_J}{2}(|n\rangle\langle n+1| + |n+1\rangle\langle n|), \quad (45)$$

where  $n$  is the number of Cooper-pairs charging the junction, and, here and below,  $q$  is the charge (in units of  $2e$ ) injected into the junction from external circuit. Eigenstates of the Hamiltonian (45) form energy bands as functions of the injected charge  $q$ , which can be varied continuously. Variations of the injected charge  $q$  within these bands leads to the possibility of controlling the tunneling of individual Cooper pairs<sup>45</sup>.

The best way of injecting the charge  $q$  in a junction is provided by the “Cooper-pair box” system<sup>46,47</sup> in which the junction is attached to external bias voltage  $V_g$  through a capacitor. If  $q$  is fixed at half of a Cooper-pair charge,  $q \simeq 1/2$ , and the tunneling amplitude  $E_J/2$  is much less than  $E_C$ , the two states of the Hamiltonian (45):  $n = 0$  and  $n = 1$  are nearly-degenerate and separated by the large energy gaps from all other states. In this regime, the junction dynamics is equivalent to that of a regular quantum two-state system with the two basis state that correspond to a Cooper pair being on the left or on the right electrode of the junction. Coherent

superposition of charge states in such a two-state system is observed indirectly by measuring either the width of the transition region between the two charge states<sup>48</sup> or the energy gap between the eigenstates<sup>49</sup> as functions of the induced charge  $q$ . Quantum coherent oscillations between the two charge states were also observed directly in the time-dependent measurement<sup>10</sup>.

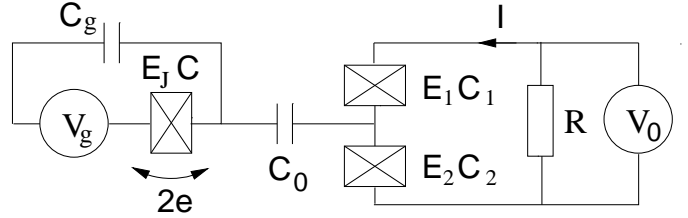


FIG. 4. Schematic diagram of a continuous measurement of the quantum oscillations of a Cooper-pair in a small Josephson junction biased with charge  $V_g C_g \simeq e$  through a small capacitance  $C_g$ . Capacitance  $C_0$  couples the oscillating Cooper pair weakly to an electrometer composed of two junctions with Josephson coupling energies  $E_{1,2}$  and capacitances  $C_{1,2}$ . The electrometer is biased with a voltage  $V_0$ , while the tunneling current  $I$  through it is the measurement output.

The experiment<sup>10</sup> was effectively based on the strong measurement of charge oscillations, when each measurement suppresses the oscillations, and they are observed as oscillations of probability in an ensemble of measurements. Continuous weak measurement of the quantum-coherent charge oscillations similar to the measurement of the flux oscillations with a dc SQUID discussed above would provide a less intrusive way of studying these oscillations. One of the detectors appropriate for such a measurement is a Cooper-pair electrometer<sup>31,50</sup>: two small Josephson junctions with Josephson coupling energies  $E_{1,2}$  and capacitances  $C_{1,2}$  connected in series and shunted with a resistor  $R$  (Fig. 4). As in the case of dc SQUID, we consider dynamics of the Cooper pair transfer through the electrometer in the regime of incoherent tunneling. The main difference with the SQUID case is that now the amplitude of Cooper pair tunneling is modulated through the modulation of energy of the intermediate state in the process of the two-step transfer of Cooper pairs in the two junctions. At small bias voltages  $V_0 \ll E_C/e$ , where from now on  $E_C = 2e^2/(C_1 + C_2)$  is the charging energy of the central electrode of the electrometer, the intermediate state is virtual, and the average current  $\langle I \rangle$  through the electrometer is determined by the same eq. (38) with  $I^{(+)}(\Theta)$  replaced with the amplitude  $I(q)$  of Cooper-pair transfer through both junctions (defined below). The charge  $q$  injected into the central electrode controls the energy of the intermediate states in the process of the Cooper-pair transfer and modulates the tunneling amplitude. At small Josephson coupling energies  $E_{1,2} \ll E_C$ , and away from the resonance points  $q = \pm 1/2$ , Cooper-pair tunneling can be treated as perturbation. Then the instantaneous value of the current  $I$  for a fixed value of the Josephson phase  $\varphi$  across the

electrometer (see, e.g., description of the two-junction system in<sup>51</sup>) is:

$$I = I(q) \sin(2eV_0t + \varphi(t)), \quad (46)$$

$$I(q) \equiv \frac{eE_1E_2}{E_C} \left( \frac{1}{1-2q} + \frac{1}{1+2q} \right).$$

The two terms in the second equation in (46) correspond to the two intermediate states with different charges  $n = \pm 1$  on the central electrode of the electrometer in the Cooper-pair transfer process.

Averaging eq. (46) over the equilibrium quantum fluctuations of  $\varphi$  we get expression for the average value of the current  $I$  that is equivalent to eq. (38). Since the tunneling current  $I$  through the electrometer is the measurement output, this expression determines the response coefficient  $\lambda$  of the electrometer:

$$\lambda \equiv (\partial\langle I \rangle / \partial q) = \pi(\partial[I(q)]^2 / \partial q)\tau/e, \quad (47)$$

where  $\tau$  is given by eqs. (39) and (40). Similarly, the output noise of the current  $I$  can be obtained as

$$S_I = [I(q)]^2 \tau'. \quad (48)$$

The backaction noise of the Cooper-pair electrometer is created by fluctuations of the charge on its central electrode in the process of the Cooper-pair tunneling. This fluctuations lead to fluctuations of electric potential of this electrode. In the same regime as for eq. (46), the magnitude of this fluctuations is determined by the magnitude of the instantaneous value of the potential at a fixed Josephson phase difference  $\varphi$  across the electrometer:

$$V = U(q) \cos(2eV_0t + \varphi(t)), \quad (49)$$

where

$$U(q) \equiv \frac{E_1E_2}{2eE_C} \left( \frac{1}{(1-2q)^2} - \frac{1}{(1+2q)^2} \right).$$

As before, averaging over the fluctuations of  $\varphi(t)$  we get the spectral density of the backaction noise and its correlation with the output noise:

$$S_V = [U(q)]^2 \tau', \quad S_{VI} = -iU(q)I(q)\tau'. \quad (50)$$

Equations (47), (48), and (50) show that at vanishing temperature, when  $\tau' = \tau$ , the noise characteristics of the Cooper-pair electrometer satisfy the general relations (7) and (4) of a quantum-limited detector. Moreover, the electrometer is “symmetric” detector in a sense that the input-output correlator  $S_{VI}$  is purely imaginary. This means that both its energy sensitivity  $\epsilon$  and the signal-to-noise ratio (29) for measurement of the two-state system reach fundamental limits.

In summary, the examples of specific detectors considered in this Section show explicitly that many standard

detectors should be capable of reaching the fundamental limits of sensitivity for measurements of electric charge and magnetic flux. In this regime, they are characterized by the fundamental signal-to-noise ration of 4 for continuous weak measurement of the macroscopic quantum coherent oscillations. The limitation on the signal-to-noise ratio of such a measurement has the same origin as the quantum limitation on the operation of an ideal linear phase-insensitive amplifier that adds a minimum of half-a-quantum of noise to the amplified signal.

The author would like to acknowledge discussions with M.H. Devoret, J.R. Friedman, A.N. Korotkov, K.K. Likharev, J.E. Lukens, Yu.V. Nazarov, R.J. Schoelkopf, G. Schön, and A.B. Zorin. This work was supported in part by AFOSR.

## Appendix

In this Appendix, we derive eq. (32) that relates the matrix elements of the perturbation of the scattering potential to the transmission properties of a point contact. Relation (32) can be established considering the stationary states of an electron confined to move on the interval  $x \in [-L/2, L/2]$  with the main scattering potential located at the center of the interval,  $x \simeq 0$ . The scattering matrix  $S$  for the symmetric scattering potential can be written as

$$S = e^{i\Theta} \begin{pmatrix} i \sin \nu, & \cos \nu \\ \cos \nu, & i \sin \nu \end{pmatrix},$$

where  $\Theta$  is the phase of the transmission amplitude, and  $\nu$  parametrizes transmission probability  $D$ :

$$D = \cos^2 \nu. \quad (51)$$

Diagonalizing the scattering matrix  $S$ , we find the two phase shifts  $\varphi_{1,2}$  associated with it:  $\varphi_1 = \Theta + \nu$ ,  $\varphi_2 = \Theta + \pi - \nu$ . The variations  $\delta\varphi_j$  of the two phase shifts due to perturbation of the scattering potential lead to changes  $\delta\varepsilon_j$  in energies of the two stationary states,

$$\delta\varepsilon_j = v_F \delta\varphi_j / L \quad (52)$$

For symmetric main scattering potential, the two stationary states  $\chi_j(x)$  are given by the even and odd combinations of the scattering states  $\psi_j(x)$ . In the basis of the states  $\chi_j$ , the perturbation matrix  $U$  introduced in eq. (30) is:

$$U = \begin{pmatrix} (U_{11} + U_{22})/2 + \text{Re}U_{12}, & (U_{11} - U_{22})/2 - i\text{Im}U_{12} \\ (U_{11} - U_{22})/2 + i\text{Im}U_{12}, & (U_{11} + U_{22})/2 - \text{Re}U_{12} \end{pmatrix}. \quad (53)$$

The diagonal elements of this matrix give the first-order corrections to the energies of the stationary states. Comparing expressions for the energy corrections given by eq. (53) to expressions for the phase shifts combined with eq. (52), we see that

$$\text{Re}U_{12} = v_F \delta \nu / L.$$

This equation, together with the relation (51) between  $\nu$  and transmission probability  $D$ , gives eq. (32) of the main text. Since the matrix (53) should be symmetric for the perturbation of the scattering potential that is symmetric with respect to the main part of the potential, we also see that  $\text{Im}U_{12} = 0$  in the symmetric case. This means that the nonvanishing imaginary part of  $U_{12}$  can be viewed as a measure of the asymmetry of coupling between the point contact and a source of the perturbation.

---

<sup>1</sup> M. Brune, E. Hagley, J. Dreyer, X. Matre, A. Maali, C. Wunderlich, J.M. Raimond, and S. Haroche, *Phys. Rev. Lett.* **77**, 4887 (1996).

<sup>2</sup> M. Arndt, O. Nairz, J. Vos-Andreae, C. Keller, G. van der Zouw, and A. Zeilinger, *Nature* **401**, 680 (1999).

<sup>3</sup> R. Rouse, S. Han, and J.E. Lukens, *Phys. Rev. Lett.* **75**, 1614 (1995).

<sup>4</sup> P. Silvestrini, V.G. Palmieri, B. Ruggiero, and M. Russo, *Phys. Rev. Lett.* **79**, 3046 (1997).

<sup>5</sup> L.J. Geerligs, D.V. Averin, and J.E. Mooij, *Phys. Rev. Lett.* **65**, 3037 (1990).

<sup>6</sup> D.V. Averin, A.N. Korotkov, A.J. Manninen, and J.P. Pekola, *Phys. Rev. Lett.* **78**, 4821 (1997).

<sup>7</sup> J.R. Friedman, M.P. Sarachik, J. Tejada, and R. Ziolo, *Phys. Rev. Lett.* **76**, 3830 (1996).

<sup>8</sup> L. Thomas, F. Lioni, R. Ballou, D. Gatteschi, R. Sessoli, and B. Barbara, *Nature* **383**, 145 (1996).

<sup>9</sup> W. Wernsdorfer, E. Bonet Orozco, K. Hasselbach, A. Benoit, D. Mailly, O. Kubo, H. Nakano, and B. Barbara, *Phys. Rev. Lett.* **79**, 4014 (1997).

<sup>10</sup> Y. Nakamura, Yu.A. Pashkin, and J.S. Tsai, *Nature* **398**, 786 (1999).

<sup>11</sup> A.J. Leggett and A. Garg, *Phys. Rev. Lett.* **54**, 857 (1985).

<sup>12</sup> D.D. Awschalom, J.F. Smyth, G. Grinstein, D.P. DiVincenzo, and D. Loss, *Phys. Rev. Lett.* **68**, 3092 (1992); **71**, 4279 (E) (1993).

<sup>13</sup> N.V. Prokof'ev and P.C.E. Stamp, *J. Phys.: Condens. Matter* **5**, L633 (1993).

<sup>14</sup> A. Garg, *Phys. Rev. Lett.* **74**, 1458 (1995); *Czech. J. Phys.* **46**, Suppl. 4, 1854 (1996).

<sup>15</sup> D.V. Averin, *Solid State Commun.* **105**, 659 (1998).

<sup>16</sup> Yu. Makhlin, G. Schön, and A. Shnirman, *Nature* **398**, 305 (1999).

<sup>17</sup> L.B. Ioffe, V.B. Geshkenbein, M.V. Feigel'man, A.L. Fauchère, and G. Blatter, *Nature* **398**, 679 (1999).

<sup>18</sup> J.E. Mooij, T.P. Orlando, L. Levitov, Lin Tian, Caspar H. van der Wal, and Seth Lloyd, *Science* **285**, 1036 (1999).

<sup>19</sup> L.E. Ballentine, *Phys. Rev. Lett.* **59**, 1493 (1987).

<sup>20</sup> A. Peres, *Phys. Rev. Lett.* **61**, 2019 (1988).

<sup>21</sup> C.D. Tesche, *Phys. Rev. Lett.* **64**, 2358 (1990).

<sup>22</sup> Y. Aharonov, D.Z. Albert, and L. Vaidman, *Phys. Rev. Lett.* **60**, 1351 (1988).

<sup>23</sup> V.B. Braginsky and F.Ya. Khalili, *Quantum measurement*, (Cambridge, 1992).

<sup>24</sup> M.B. Mensky, *Phys. Usp.* **41**, 923 (1998).

<sup>25</sup> A.N. Korotkov and D.V. Averin, *cond-mat/0002203*.

<sup>26</sup> S. Han, J. Lapointe, and J.E. Lukens, *Phys. Rev. Lett.* **66**, 810 (1991).

<sup>27</sup> U. Weiss, *Quantum dissipative systems*, (World Scientific, 1993).

<sup>28</sup> J. Clarke, C.D. Tesche, and R.P. Giffard, *J. Low Temp. Phys.* **37**, 405 (1979).

<sup>29</sup> V.V. Danilov, K.K. Likharev, and O.V. Snigirev, in: *SQUID'80*, ed. by H.-D. Hahlbohm and H. Lübbig, (Berlin, W. de Gruyter, 1980), p. 473.

<sup>30</sup> V.V. Danilov, K.K. Likharev, and A.B. Zorin, *IEEE Trans. Magn.* **19**, 572 (1983).

<sup>31</sup> A.B. Zorin, *Phys. Rev. Lett.* **76**, 4408 (1996).

<sup>32</sup> C.M. Caves, *Phys. Rev. D* **26**, 1817 (1982).

<sup>33</sup> M. Field, C.G. Smith, M. Pepper, D.A. Ritchie, J.E.F. Frost, G.A.C. Jones, and D.G. Hasko, *Phys. Rev. Lett.* **70**, 1311 (1993).

<sup>34</sup> M. Kataoka, C.J.B. Ford, G. Faini, D. Mailly, M.Y. Simmons, D.R. Mace, C.-T. Liang, and D. A. Ritchie, *Phys. Rev. Lett.* **83**, 160 (1999).

<sup>35</sup> E. Buks, R. Schuster, M. Heiblum, D. Mahalu, and V. Umansky, *Nature* **391**, 871 (1998).

<sup>36</sup> D. Sprinzak, E. Buks, M. Heiblum, and H. Shtrikman, *cond-mat/9907162*.

<sup>37</sup> S.A. Gurvitz, *Phys. Rev. B* **56**, 15215 (1997).

<sup>38</sup> Y. Levinson, *Europhys. Lett.* **39**, 299 (1997).

<sup>39</sup> I.L. Aleiner, N.S. Wingreen, and Y. Meir, *Phys. Rev. Lett.* **79**, 3740 (1997).

<sup>40</sup> G. Hackenbroich, B. Rosenow, and H. A. Weidenmüller, *Phys. Rev. Lett.* **81**, 5896 (1998).

<sup>41</sup> M. Büttiker and A. M. Martin, *Phys. Rev. B* **61**, 2737 (2000).

<sup>42</sup> A.N. Korotkov, *Phys. Rev. B* **60**, 5737 (1999).

<sup>43</sup> D.V. Averin, Yu.V. Nazarov, and A.A. Odintsov, *Physica B* **165&166**, 945 (1990).

<sup>44</sup> G.-L. Ingold and Yu.V. Nazarov, in: *"Single Charge Tunneling"*, ed. by H. Grabert and M.H. Devoret (Plenum, New York, 1992), p. 21.

<sup>45</sup> D.V. Averin, A.B. Zorin, and K.K. Likharev, *Zh. Eksp. Teor. Fiz.* **88**, 692 (1985) [Sov. Phys. JETP **61**, 407].

<sup>46</sup> M. Büttiker, *Phys. Rev. B* **36**, 3548 (1987).

<sup>47</sup> P. Lafarge, H. Pothier, E.R. Williams, D. Esteve, C. Urbina, and M.H. Devoret, *Z. Phys. B* **85**, 327 (1991).

<sup>48</sup> V. Bouchiat, D. Vion, P. Joyez, D. Esteve, and M.H. Devoret, *J. of Supercond.* **12**, 789 (1999).

<sup>49</sup> D.J. Flees, S. Han, and J.E. Lukens, *J. of Supercond.* **12**, 813 (1999).

<sup>50</sup> A.B. Zorin, S.V. Lotkhov, Yu.A. Pashkin, H. Zangerle, V.A. Krupenin, T. Weimann, H. Schere, and J. Niemeyer, *J. of Supercond.* **12**, 747 (1999).

<sup>51</sup> D.V. Averin and K.K. Likharev, in: *"Mesoscopic Phenomena in Solids"*, ed. by B.L. Altshuler et al. (Elsevier, Amsterdam, 1991), p. 173.